

UNCLASSIFIED

Defense Technical Information Center  
Compilation Part Notice

ADP011012

TITLE: Structural and Optical Properties of Gold in MgO: Effects of Shape and the Interface

DISTRIBUTION: Approved for public release, distribution unlimited

This paper is part of the following report:

TITLE: Materials Research Society Symposium Proceedings Volume 635.  
Anisotropic Nanoparticles - Synthesis, Characterization and Applications

To order the complete compilation report, use: ADA395000

The component part is provided here to allow users access to individually authored sections of proceedings, annals, symposia, etc. However, the component should be considered within the context of the overall compilation report and not as a stand-alone technical report.

The following component part numbers comprise the compilation report:

ADP011010 thru ADP011040

UNCLASSIFIED

## Structural and Optical Properties of Gold In MgO: Effects of Shape And The Interface

Elana M. Bryant, Akira Ueda, Richard R. Mu, Marvin H. Wu, Alkiviathes Meldrum<sup>1</sup> and Don O. Henderson

Chemical Physics Laboratory, Department of Physics, Fisk University, Nashville, TN 37208, USA  
<sup>1</sup>Department of Physics, University of Alberta, Edmonton, Alberta, Canada

### ABSTRACT

The fundamental studies of metallic nanoparticles embedded in various host materials have been made. The host-guest interaction causes the shapes of embedded nanoparticles, and the surface plasmon resonances of the metallic nanoparticles are affected by the host materials. The control of the surface plasmon resonance condition is a challenging question. We will discuss the interface effect of the systems where gold nanoparticles were fabricated between materials of MgO and SiO<sub>2</sub>.

### INTRODUCTION

Surface plasmon resonance (SPR) of small metallic particles has been studied since Mie's idea of 1908 about the study [1] of optical properties of gold particles, and in the past three decades the new field of cluster science has been developed with many potential applications. Although many studies have been published, there are still new interesting systems and there are fundamental questions to be answered. In our laboratory, we have studied the systems of several insulating materials implanted with gold ions (Al<sub>2</sub>O<sub>3</sub>:Au, CaF<sub>2</sub>:Au, Silica SiO<sub>2</sub>:Au, MgO: Au, Muscovite Mica: Au, and Vycor Glass: Au) and of the porous materials impregnated with gold (Vycor Glass: Au)[2-5].

In the systems of SiO<sub>2</sub>:Au and MgO: Au fabricated by ion implantation, we have previously seen the growth of gold nanocrystals and found the SPR positions to be 530 nm and 560 nm, respectively, after a suitable thermal annealing in 5%O<sub>2</sub>+95%Ar atmosphere. These SPR positions agree with the Mie's theory using a dipole approximation for spherical particles, that satisfies the following equation [6]:

$$\varepsilon(\omega_{sp}) + 2\varepsilon_m = 0, \quad (1)$$

where  $\varepsilon(\omega)$  is the dielectric function of gold,  $\varepsilon_m$  is the dielectric function of host material, and  $\omega_{sp}$  is the surface plasmon frequency.

As shown in figure 1, from our previous experiments, the gold nanocrystals in MgO have cubic shape, that aligns along the crystal axis of MgO (100), while the gold nanocrystals in SiO<sub>2</sub> are spherical. (The detail of this result will be discussed elsewhere.) If only the surface energy of gold particles plays the

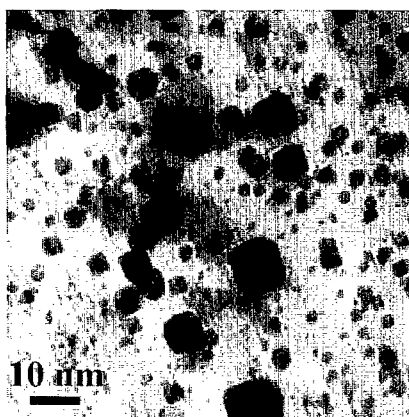


Figure 1 TEM image of Gold nanocrystals fabricated in MgO single crystal by ion implantation with a post annealing. The shape of the gold nanocrystals is cubic and they align along the crystal axis of host MgO (100).

dominant role for the nanocrystal growth, the shape should be spherical. The host MgO crystal, therefore, must contribute to this result of cubic gold particles because MgO single crystal has a cubic crystal structure.

In this paper, we will discuss the interfacial interaction between gold nanocrystals and the dielectric hosts, in terms of dielectric constants and the crystal-amorphous character of host, by observing the SPR band of the system. In order to see the matrix dependence, we fabricated the following four systems: (1)Au deposited on MgO substrate with a MgO overcoat [MAM], (2)Au deposited on SiO<sub>2</sub> substrate with a MgO overcoat [SAM], (3)Au deposited on MgO substrate with a SiO<sub>2</sub> overcoat [MAS], and (4)Au deposited on SiO<sub>2</sub> substrate with a SiO<sub>2</sub> overcoat [SAS]. Hereafter, the abbreviations for the systems MAM, SAM, MAS, and SAS will be used for simplicity: the each letter in the abbreviations from left to right represents the substrate material, gold deposition, and the overcoat materials, respectively.

## EXPERIMENTAL

MgO substrates were single crystal plates (1" x 1" x 0.5 mm) with polished (100) surface obtained from Princeton Scientific Corporation. SiO<sub>2</sub> substrates were Corning 7940 optical grade Fused silica glass windows. Gold was deposited onto the substrates in a vacuum with the pressure of  $\sim 10^{-7}$  torr by the pulsed laser deposition method with a pico-second Nd:YAG laser. The used wavelength was 532 nm, which was the second harmonic of Nd:YAG laser. The laser beam energy was controlled with a cross polarizer. The used energy was 100  $\mu$ J per pulse with 10 Hz repetition rate for 60 min. Overcoating was carried out by electron beam evaporation with thickness of 100 nm and a deposition rate of 1.5  $\text{\AA}/\text{sec}$  for both SiO<sub>2</sub> and MgO in a vacuum of  $\sim 10^{-7}$  torr. UV-Visible spectra of the samples were taken before and after every thermal annealing with a Hitachi spectrophotometer. Thermal annealing was made with a tube furnace with Ar gas (99.995%) flow.

## RESULTS AND DISCUSSIONS

Figure 2 shows the annealing temperature dependence of the UV-V absorbance spectra for four systems. Each spectrum was taken from a different sample annealed isothermally at a certain temperature as indicated. Since each sample may have a variance in gold density and in the thickness of overcoat materials, there should exist some fluctuation among spectra. However, according to these spectra, there are obvious differences and tendency among spectra for four types of systems. In general, at low annealing temperatures, there are SPR absorption bands tailing into longer wavelength because the prepared sample consists of an island-type gold film and the gold film may not be ruptured at low temperatures. The SPR bands became sharper as the annealing temperature increased, which indicates that the gold film had been ruptured and formed nano-meter size gold particles in the system. For the system with MgO overcoat (MAM and SAM), the SPR band dramatically decreased at the temperature greater than 1000°C, which indicated gold atoms escaped from the system through the thin overcoat with a thickness of 100 nm.

In Figure 3, the annealing temperature dependence of SPR peak position is shown, abstracted from the spectra in figure 2. For the system with MgO overcoat (MAM and SAM), SPR bands shifted to longer wavelength side at 400°C, while SPR positions for the system with SiO<sub>2</sub> overcoat (MAS and SAS) stayed up to the temperature below 700°C. At 600°C, for the system with MgO overcoat (MAM and SAM), SPR bands shifted to shorter wavelength side up to the temperature of 1000°C in the similar way, although the SPR positions themselves were different. Since gold atoms in MAM and SAM may have escaped above 1000°C, it is difficult to compare these four type systems. For the system with SiO<sub>2</sub> overcoat, SAS and MAS, above 900°C, the SPR

for MAS shifted to longer wavelength, while SPR for SAS shifted to shorter wavelength. The final SPR position for SAS (536 nm) is close to the SPR position 531-535 nm for the system of  $\text{SiO}_2$  implanted with gold with post annealing. On the other hand, the SPR positions for the systems related to MgO substrate (MAM and MAS) were both longer wavelength side than the SPR position 560 nm for the system of MgO implanted with gold with post annealing. For the system of MAM, before the SPR band became weak at 900°C, the SPR peak was located at 583 nm. This result indicates that the SPR position does not depend only on the dielectric function of the surrounding material.

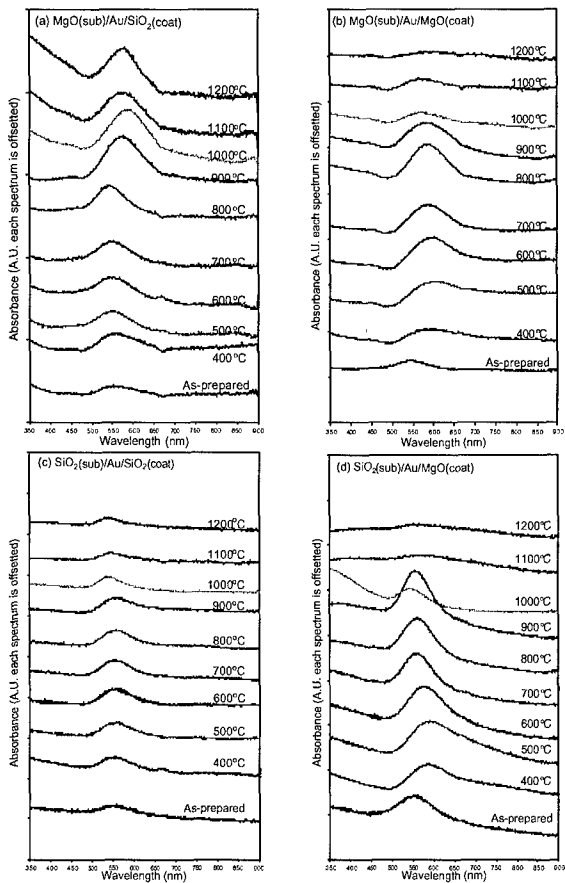


Figure 2 Overview of UV-Vis spectra for four kinds of systems: (a)  $\text{MgO}[\text{sub}]/\text{Au}/\text{SiO}_2[\text{coat}]$ , (b)  $\text{MgO}[\text{sub}]/\text{Au}/\text{MgO}[\text{coat}]$ , (c)  $\text{SiO}_2[\text{sub}]/\text{Au}/\text{SiO}_2[\text{coat}]$ , and (d)  $\text{SiO}_2[\text{sub}]/\text{Au}/\text{MgO}[\text{coat}]$ .

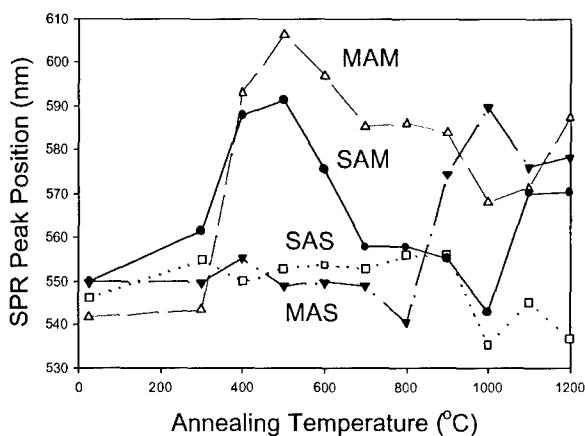


Figure 3 The annealing temperature dependence of SPR for four-types of system

Since there is a possibility to have anisotropic gold particles in the system, especially system MAM, we have measured transmission spectra of MAM using polarized light in two different geometry as shown in Figure 4. The first configuration (a) is for the absorption measurement of anisotropic gold particles by rotating the polarization plane relative to the crystal axis of MgO with normal incident. The second configuration (b) is for the absorption measurement of anisotropic gold particles by changing the incident angle with p-polarized light. The results are shown in Figure 5: Figure 5(a) shows transmission spectra in which there are no significant changes while the polarization plane rotates relative to crystal axis. Figure 5(b) shows the some effect of change in the incident angle on the SPR position, which suggests that there exists some anisotropy in the system although the reflection loss depends on incident angle and wavelength, which may cause shift of the SPR position.

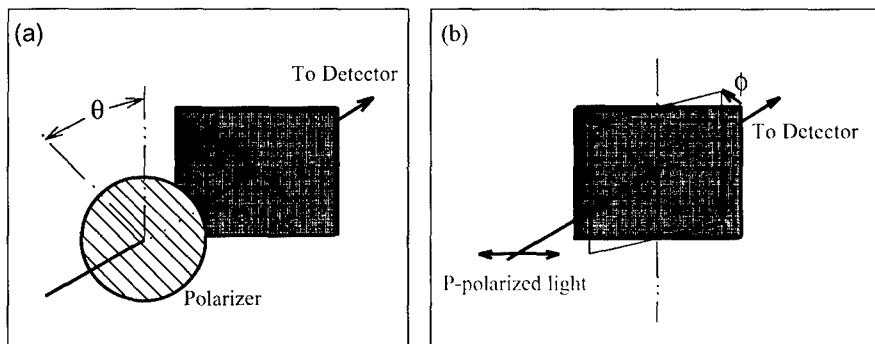


Figure 4 Two configurations for transmission measurements using polarized light

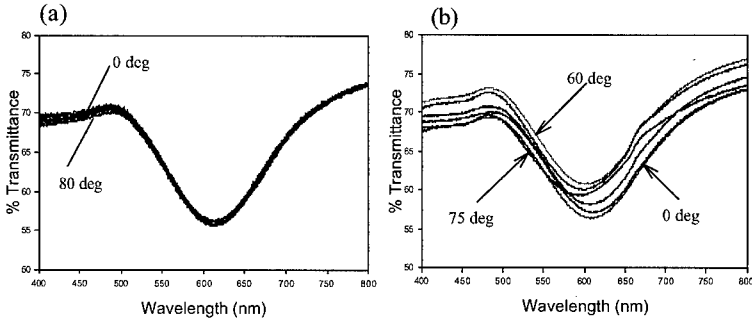


Figure 5 The transmission spectra for two types of configuration as shown in Figure 4 (a) and (b), respectively.

Figure 5(a) suggests that the gold particles have spherical symmetry around the axis normal to the interface and Figure 5(b) suggests that the gold particles have oblate spheroid shape (pancake shape) with a minor axis normal to the interface. Although the spectra in Figure 5(a) did not show the change due to the rotation of polarization, this does not mean that the gold particles do not have anisotropic shapes within the interface plane. The absorption cross-section due to a prolate spheroid (cigar shape) lying in the interface is given by [Warmack]

$$\sigma(\theta) = \frac{2\pi}{\lambda} \text{Im}(\alpha_x \cos^2 \theta + \alpha_y \sin^2 \theta) \quad (2)$$

where the polarizability  $\alpha_i$ 's and depolarization factors  $n_i$  are given by, with the assumption that the major axis of prolate spheroid is y-component and the minor axis is x-component with the eccentricity of  $e$ ,

$$\text{Im} \alpha_i = \frac{\epsilon_2 \epsilon_m n_i}{[\epsilon_m + (\epsilon_1 - \epsilon_m) n_i]^2 + (\epsilon_2 n_i)^2} V \quad (3)$$

$$n_y = \frac{1-e^2}{2e^3} \left( Ln \frac{1+e}{1-e} - 2e \right) \text{ and } n_x = \frac{1}{2}(1-n_y). \quad (4)$$

Here the angle  $\theta$  is taken between the major axis of spheroid and the polarization of the incident light, and  $V$  is the volume of the gold particle. If 50% of prolate spheroids distribute in (100) direction and the other 50% distribute in (010) direction, then the total absorption cross-section becomes

$$\bar{\sigma}(\theta) = \frac{2\pi}{\lambda} \text{Im} \left[ \frac{1}{2}(\alpha_x \cos^2 \theta + \alpha_y \sin^2 \theta) + \frac{1}{2}(\alpha_x \sin^2 \theta + \alpha_y \cos^2 \theta) \right] = \frac{\pi}{\lambda} \text{Im}[\alpha_x + \alpha_y]. \quad (5)$$

This does not effectively depend on the angle  $\theta$ , so that we may not have seen the polarization dependence. In order to see the particle shapes, the direct measurement of the particle shape is necessary with TEM, and TEM measurements are in the process.

According to the comparison among the four-type systems (MAM, MAS, SAM, and SAS), SAS system probably has spherical gold because we saw SPR around 530 nm, while the other systems may have anisotropic gold particles. For SAS, the coated SiO<sub>2</sub> fuses to the substrate SiO<sub>2</sub> during the annealing, and then gold particles could relax to form spherically shaped particles. For the hetero-system, MAS and SAM, the coated material would not fuse to the substrate material, and then the shape of gold particle remains anisotropic, which is most likely oblate spheroid shape. For homo-system, MAM, we may have prolate spheroid as well as oblate spheroid.

There may have other possibilities to explain the spectra, one of which is the aggregation of gold particles. Before annealing, an imperfect gold film was formed by laser ablation, which consists of many small gold particles. A particle can interact with the other particles through the induced dipole moments as long as the distance between particles is short enough. This interaction causes other modes locating at longer wavelengths.

## Conclusion

We have proposed a fabrication method to produce a system of anisotropic gold nanoparticles, which may control the SPR position. For the fundamental point of view, it is interesting to see the effect of materials that contact gold particles in these systems.

## Reference

- [1]G. Mie, Ann, Physik **25**, 377(1908). (German)
- [2]D.O. Henderson, Y.-S. Tung, A. Ueda, R. Mu, Y. Xue, C. Hall, W.E. Collins, C.W. White, R.A. Zuhr, Jane G. Zhu, and P.W. Wang, J. of Vacuum Science and Technology **A 14**(3), 1199(1996); D.O. Henderson, Y.-S. Tung, R. Mu, A. Ueda, J. Chen, R. Gu, C.W. White, Jane G. Zhu, M. McKay, and O. Scott., International Conference of Defects in Insulating Materials, Wake Forest University, Winston-Salem, NC, USA, 1996. Materials Science Forum **239-241**, 695(1997).
- [3]Z. Gu, R. Mu, A. Ueda, Y.-S. Tung, M.H. Wu, D.O. Henderson, A. Meldrum, C.W. White, and R.A. Zuhr, JVST **A16**(3), 1409(1998).
- [4]A. Ueda, D.O. Henderson, R. Mu, Y.-S. Tung, C.W. White, Jane G. Zhu, International Conference of Defects in Insulating Materials, Wake Forest University, Winston-Salem, NC, USA, 1996. Materials Science Forum **239-241**, 675(1997); A. Ueda, R. Mu, Y.-S. Tung, M. H. Wu, W.E. Collins, D.O. Henderson, C.W. White, R.A. Zuhr, J.D. Budai, A. Meldrum, P.W. Wang, and Xi Li, Nucl. Instru. Mater. Method in Phys. Res. **B 141** 261(1998).
- [5]D.O. Henderson, R. Mu, A. Ueda, Y.-S. Tung, C.W. White, R.A. Zuhr, and Jane G. Zhu, J. of Non-Crystalline Solids, **205/207**, 788(1996). The Ninth International Conference on Liquid and Amorphous Metal, Chicago, IL October 8-13, 1995, Proceedings; Y.-S. Tung, R. Mu, D.O. Henderson, A. Ueda, C.W. White, Jane G. Zhu, International Conference of Defects in Insulating Materials, Wake Forest University, Winston-Salem, NC, USA, 1996. Materials Science Forum **239-241**, 691(1997).
- [6]U. Kreibig and M. Vollmer, "Optical Properties of Metal Clusters," Springer Series in Materials Science **25** (Springer, New York, 1995).
- [7]P. Clippe, R. Evrard, and A.A. Lucas, Phys. Rev. B14, 1715(1976); M. Ausloos and P. Clippe, Phys. Rev. **B18**, 7176(1978).

**Metallic Nanoparticles  
and Clusters II**